Earth and Planetary Science Letters 276 (2008) 30–39

Contents lists available at ScienceDirect

Earth and Planetary Science Letters

journal homepage: www.elsevier.com/locate/epsl

Re–Os isotopic compositions of picrites from the Emeishan flood basalt province, China

Zhaochong Zhang [a,*], Xiachen Zhi [b], Lei Chen [b], Andrew D. Saunders [c], Marc K. Reichow [c]

[a] State Key Laboratory of Geological Processes and Mineral Resources, China University of Geosciences, Beijing, 100083, China
[b] CAS Key Laboratory of Crust–Mantle Materials and Environment, School of Earth and Space Sciences, University of Science and Technology of China, Hefei, 230026, China
[c] Department of Geology, University of Leicester, Leicester LE1 7RH, UK

ARTICLE INFO

Article history:
Received 23 January 2008
Received in revised form 29 August 2008
Accepted 2 September 2008
Available online 18 October 2008

Editor: R.W. Carlson

Keywords:
Re–Os isotope
picrite
plume
Emeishan flood basalt province
upper–lower mantle boundary

ABSTRACT

Picrites from the Lijiang area, in the western part of the Emeishan flood basalt province, are considered to be one of the most important indicators of the Emeishan mantle plume, and may represent initial mantle plume activity. This paper presents the first Re–Os isotope data for picrites from the province. Eighteen geochemically well characterised samples, including 12 picrites and 6 basalts from two sections near Lijiang, have been analyzed for Os isotopes. The picrites from the two sections have overlapping Re and Os concentrations and initial Os isotopic compositions. They have higher Os concentrations (1.5–3 parts per billion), and slightly lower Re concentrations (<0.07 ppb) than those from many other flood basalt provinces (FBPs) and ocean island picrites. The picrites have distinctly unradiogenic Os isotopes with $\gamma_{Os}(t)$ values (t=259 Ma) of −0.9 to −2.4, but the associated basalts have suprachondritic Os isotope compositions with $\gamma_{Os}(t)$ of 1.8 to 73.3, which overlap with published data for basalts from other localities in the province. The high $\gamma_{Os}(t)$ values of the basalts could be the result of crustal contamination, which is enabled by the low Os concentrations in the parental basalts. The low $\gamma_{Os}(t)$ values of the picrites are unusual in terms of plume-related magmatism. There is no clear evidence for recycled crustal material in the mantle source of the Emeishan picrites, or for a significant degree of interaction of the picrites with ancient subcontinental lithospheric mantle of the Yangtze craton. The low $\gamma_{Os}(t)$ values relative to many other plume-related picrites (from ocean islands or flood basalt provinces) indicate that there was no clear Os isotope evidence of involvement of the Earth's core or recycled crustal components in the formation of Emeishan flood basalt province.

1. Introduction

Continental flood basalt provinces (CFBs), characterized by voluminous volcanic sequences erupted in a short period of time and transient surface uplift, are thought to originate from the rapid ascent of mantle plumes (Larsen and Yuen, 1997; Larsen et al., 1999; Saunders et al., 2007). The plumes are probably derived from boundary layers, such as the interface between the upper and lower mantle (i.e. 670 km discontinuity), or the D″ layer at the core–mantle boundary (CMB, Allègre and Turcotte, 1985; Hofmann, 1997), although there has been little direct evidence for either location. Recent seismic evidence suggests that the roots of the Iceland and Hawaiian plumes may reside at the CMB, supporting the view that some plumes may originate at this interface (e.g., Bijwaard and Spakman, 1999; Helmberger et al., 1998; Russell et al., 1988; Montelli et al., 2003, 2006; Nolet et al., 2006, 2007).

Constraints on the composition and location of the source regions that ultimately give rise to mantle plumes would provide important information on the structure of the deep mantle, timescales of mantle mixing and possibly interaction between the mantle and the outer core. However, incompatible elements, and Sr, Nd and Pb isotope ratios, are of limited efficiency as indicators of plume sources, because they are easily overwhelmed by continental lithospheric mantle and crust. In contrast, the chalcophile and siderophile nature of Re and Os, combined with the compatible behavior of Os during mantle melting, set this isotope system apart from conventional lithophile isotope systems and provide a unique insight into mantle plume processes. Thus, if chemical exchange occurs across the CMB, the hypothesized long-term elevation in Re/Os and Pt/Os in the outer core would impart a coupled enrichment of ^{187}Os and ^{186}Os to mantle plumes derived from the CMB. This isotopic fingerprinting might be observed in a plume, because the outer core likely has approximately 300 times higher abundances of Os than the mantle. Such coupled enrichments have been confirmed via high precision isotope analyses of picrites from Hawaii and the Permo-Triassic Siberian Traps (Walker et al., 1997; Brandon et al., 1998).

Unfortunately, many CFB lavas are crustally contaminated and/or they contain significant contributions from the subcontinental lithospheric mantle (SCLM, Ellam et al., 1992; Gallagher, and Hawkesworth,

* Corresponding author.
E-mail address: zhangzhaochong@hotmail.com (Z. Zhang).

0012-821X/$ – see front matter © 2008 Elsevier B.V. All rights reserved.
doi:10.1016/j.epsl.2008.09.005

1992; Arndt et al., 1993), making inferences about deeper (i.e., sublithospheric) mantle compositions difficult. This study presents the first Re–Os isotope data for a suite of picrites and associated basalts from the Lijiang area, in the western part of the Emeishan flood basalt province, which was previously characterized geochemically by Zhang et al. (2006a). These lavas represent early magmatism associated with the initiation of the Emeishan plume. High Os concentrations in these picritic lavas mean they are relatively insensitive to crustal contamination and therefore represent the best samples of sublithospheric (possibly plume-related) material so far analysed from this area.

2. Geological setting and timing of magmatism

The Late Permian Emeishan flood basalt province (Emeishan FBP) is exposed over a large area in southwest China (and possibly in northern Vietnam), extending from the eastern margin of the Tibetan Plateau to the western margin of the Yangtze craton (Fig. 1). The flood basalts cover an area of more than 2.5×10^5 km^2 with a diameter of ~500 km, and the thickness of the volcanic succession ranges from ~5 km in the west to ~100 m in the east (Chung and Jahn 1995; Song et al. 2001; Xu et al. 2001). The Emeishan FBP consists predominantly of a succession of tholeiites, with minor picritic and rhyolitic/trachytic flows. In addition to lava flows, mafic–ultramafic layered complexes, dikes and sills, syenite, and other alkaline intrusions, form part of the Emeishan FBP.

The lava sequence is underlain by late Carboniferous–Permian sedimentary beds atop a Mesoproterozoic to late Paleoproterozoic metamorphic basement. A recent biostratigraphic and stratigraphic investigation has shown that starting in the early Permian, thick (>1 km) carbonate sequences were deposited as a response to extensive transgression and basin subsidence in the southwest. Later, basement uplift took place, suggesting rapid kilometer-scale doming, accompanied by crustal thinning, before emplacement of the Emeishan lavas (He et al., 2003; Xu et al., 2004).

In contrast to the Siberian Traps, which formed at relatively high northern latitude, emplacement of the Emeishan flood basalts occurred near the equator (Enkin et al., 1992). Overall, the province appears to be slightly older than the much better-dated, ~251 Ma Siberian Traps. Recent U–Pb dating of zircons in the Xinjie layered mafic–ultramafic intrusion in the central part of the province yielded an age of 259±3 Ma (Zhou et al., 2002), whereas ^{40}Ar–^{39}Ar ages of 254±5 Ma (Boven et al., 2002), 255 Ma, and 251–253 Ma (Lo et al., 2002) have been reported for lava flows and two late-stage intrusions. More recent SHRIMP U–Pb dating for mafic intrusions, dykes and volcanic rocks have yielded an age range from 257 to 263 Ma (Guo et al., 2004; Zhong and Zhu, 2006; He et al., 2007; Zhou

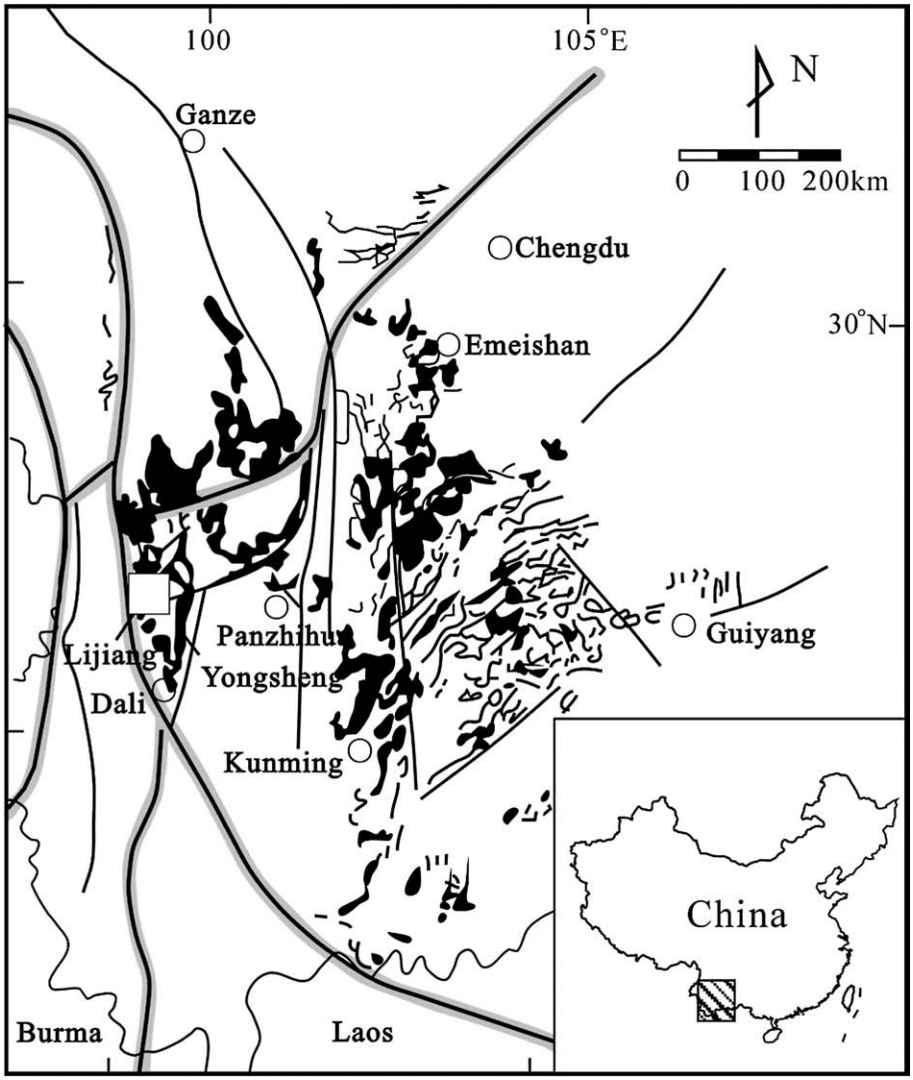

Fig. 1. Map showing principal outcrops of the Emeishan flood basalts (shown in black) (modified from Chung and Jahn, 1995). Square symbol located near Lijiang marks the sample locality.

et al., 2008), which unequivocally indicates a temporal link between the Emeishan large igneous province and the end-Guadalupian mass extinction (Middle Permian).

3. Mineralogy and petrography of the Lijiang picrites and basalts

The recently discovered picritic flows in the Lijiang area are located in an 800 m thick lava section near Shiman and a 5500 m thick section at Daju, one of the thickest in the entire Emeishan province (see Fig. 2). These two occurrences are about 26 km apart. In both sections, the picritic flows are intercalated with augite–phyric basalt flows (Fig. 2). At Shiman, the lowermost and uppermost picritic flows are 3–5 m thick, whereas a middle picritic flow is 15–20 m thick. In the Daju section, the lowermost picritic flow varies in thickness from 20 to 50 m whereas others are 3–5 m thick. The two sections differ considerably in total thickness and it is unclear how, or whether, the picritic flows at Shiman correlate with those at Daju. Massive aphyric basalt flows and, at Daju, amygdaloidal basalt dominate the middle to upper parts of the lava sections. Plagioclase-phyric basalt, abundant in other parts of the province, is absent in the studied sections.

Most of the picritic flows are highly porphyritic (with 7–15 vol.% phenocrysts). They contain abundant phenocrysts of forsteritic olivine, plus minor diopsidic clinopyroxene. The olivine phenocrysts are generally subhedral to rounded, and rarely embayed or partly resorbed. Most range from 0.2 to 1 mm across, although the largest grains reach 4 mm. Olivine is generally replaced by serpentine, but some grains retain cores of unaltered olivine (up to 91.6% Fo), many of which contain scattered melt inclusions. Strained, kink-banded crystals are absent. Some olivine crystals host equant, euhedral to rounded Cr-spinel a few tens of microns across. Cr-spinel is also present as solitary grains in the groundmass. The groundmass retains an unaltered appearance and consists principally of very fine grained, probably originally glassy, mesostasis plus lesser amounts of olivine, anhedral diopside, and small plagioclase crystals. The groundmass olivine tends to be less altered than the olivine phenocrysts; some are nearly equant, but elongated skeletal forms (as large as 0.5 mm–0.1 mm) consisting of parallel sets in optical continuity are most common. However, no sulfides have been recognized under careful observation and mineral separation by heavy liquid (Zhang et al., 2006b).

Both the porphyritic basalts and aphyric basalts are mostly unaltered. The porphyritic basalts contain 5–15 vol.% augite phenocrysts 1–6 mm across, that partially form clusters. The groundmass is fine grained, with intersertal or intergranular texture, and consists predominantly of plagioclase and augite with minor iron oxides. The aphyric basalts contain a similar assemblage of minerals. Augite microphenocrysts, several tens of microns across, are present, and commonly form glomerocrysts, producing a cumulophyric texture. The groundmass is composed of plagioclase laths with interstitial subophitic augite and minor anhedral magnetite.

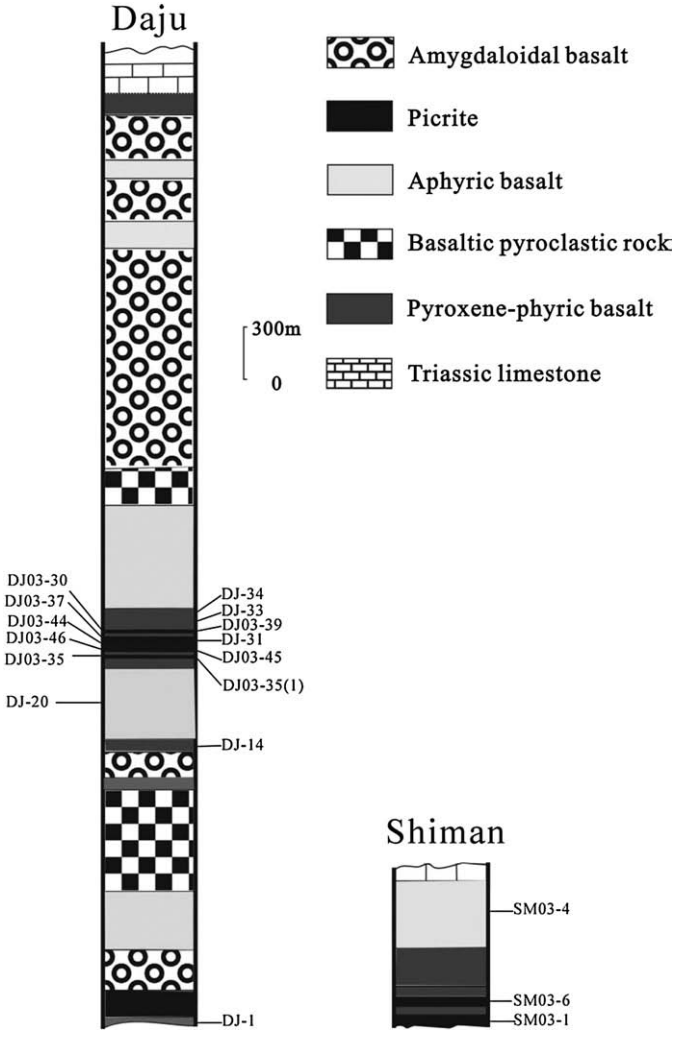

Fig. 2. Simplified stratigraphic columns of the Daju and Shiman sections, with sample numbers.

4. Analytical methods

To avoid potential Re contamination from steel and tungsten carbide crushing equipment, all whole-rock powders were prepared using a ceramic jaw crusher and agate mill at the Chinese Academy of Geological Sciences, Beijing. The jaw crusher and mill were thoroughly cleaned between samples by crushing multiple aliquots of clean quartz and pre-contaminated with an aliquot of the sample. The contaminated sample was discarded prior to preparation of a clean aliquot of rock powder.

Chemical preparation and mass spectrometric determination of all samples were conducted at the Isotope Laboratory of School of Earth and Space Sciences, University of Sciences and Technology of China (USTC). About 2 g of powder sample, ^{190}Os spike, 3 ml HCl (~12 mol/l), ^{185}Re spike, and 6 ml HNO_3 (~15 mol/l) were loaded into Carius tube in turn at low temperature (−90 °C), then digested in a sealed Carius tube protected within a steel tube at 230 °C, for about 18 h. The Carius tube was cooled and shaken in an ultrasonic vibrator for about 30 min, which was then put in a steel tube and heated at 230 °C for 18 h again.

The extraction and purification of Os were performed via a two-step distillation process modified after Nägler and Frei (1997) and Birck et al. (1997). The pure Os solution was then concentrated to about 1 μl for mass spectrometric determination. The Os isotopic composition was measured by negative thermal ionization mass spectrometry (NTIMS) on a Finnigan MAT262 mass spectrometer at USTC, using Faraday cups in static mode or ion-counting system in dynamic mode depending on signal intensity. Errors on ^{187}Os/^{188}Os ratios for most samples are less than 0.1% ($2\sigma_{SD}$). The ^{187}Os/^{188}Os ratio measured was corrected for mass fractionation and oxygen isotopic composition. The Os concentration of samples was calculated following the isotope dilution method. The liquid Os standard was frequently run for monitoring mass spectrometry during sample measurements. The Os standard run over the period of experiments gave an ^{187}Os/^{188}Os ratio of 0.17368±0.00028 ($2\sigma_{SD}$, n=9) which is within the range of 0.17386±0.00054 (2σ) reported by other laboratories (Reisberg et al., 2004).

Rhenium was separated and purified from the residues of Os extractions using AG1X8 anion exchange resin. First, the column was cleaned with 3 ml HNO_3 (0.8 mol/l), 5 ml HNO_3 (8 mol/l), 5 ml HNO_3 (8 mol/l) and 3 mL HNO_3 (0.8 mol/l) in turn. Then the residues from Os extractions were dried at 115 °C and re-dissolved in 5 mL HNO_3 (0.4 mol/l). After cooling and centrifugation (40 min) of the solution,

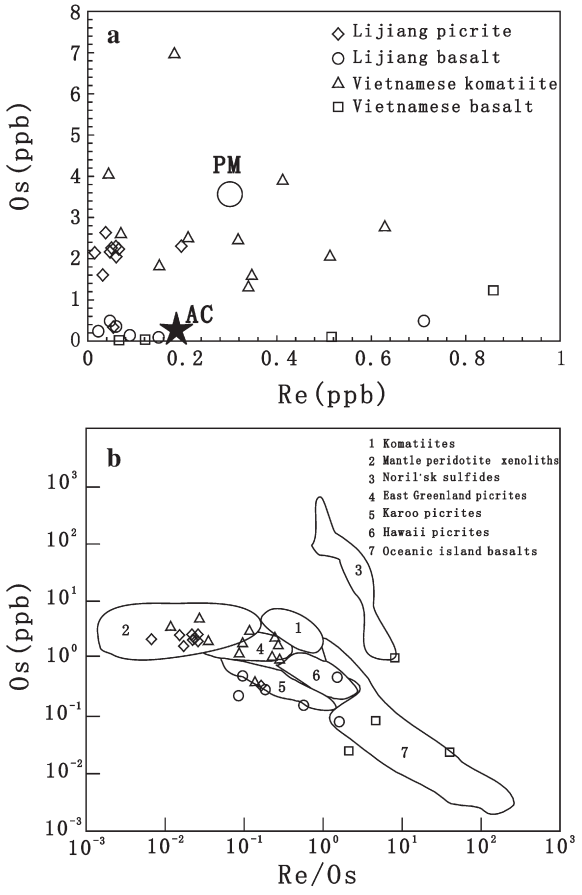

Fig. 3. (a) Re vs. Os and (b) Os vs. Re/Os (modified from Brooks et al., 1999 and references therein). PM: primary mantle (circle) (Bennett et al., 2000); AC: average crust (star) (Taylor and Mclennan, 1995). Vietnamese samples are from Hanski et al. (2004).

the upper clean solution was loaded and rinsed with 6 ml and 3 ml HNO_3 (0.8 mol/l) and eluted with 5 mL HNO_3 (8 mol/l). The eluted solution was dried at 115 °C and re-dissolved in 1 ml HNO_3 (3%). Spiked Re isotopic ratio was determined on the Finnigan MAT Element II ICP-MS at the Department of Earth Science, Nanjing University. The precision of $^{185}Re/^{187}Re$ measurement was about 1% ($2\sigma_{SD}$). The $^{185}Re/^{187}Re$ ratio of liquid Re standards of various concentrations has a mean of 0.597±0.003 (2σ), which is consistent with the known isotope ratio of Re.

The full procedure blanks (FPB) of Os and Re were 5 pg and 3 pg, respectively, during all sample determination. A laboratory standard peridotite P-16 was analyzed in 7 runs, giving Os and Re concentrations of 2.04±0.15 (2σ) ppb and 0.098±0.009 (2σ) ppb, respectively, and the $^{187}Os/^{188}Os$ ratio of 0.1219±0.0015 (2σ) which are within the ranges of the results of our laboratory during last few years. The reference material UB–N (Meisel et al., 2003) was analyzed, giving $^{187}Os/^{186}Os$ of 0.12819±0.00017 consistent with the recommended value of UB–N in error range.

Sr, Nd and Pb isotopic analyses were carried out at the Chinese Academy of Sciences, using approximately 1000 mg of hand-selected whole-rock chips. Before digestion for isotopic analysis, whole-rock samples were leached with 6 M HCl in order to remove any alteration. $^{87}Sr/^{86}Sr$ and $^{143}Nd/^{144}Nd$ ratios were determined on a VG 354 mass spectrometer, and isotopic ratios were normalized to $^{145}Nd/^{144}Nd=0.7219$ and $^{86}Sr/^{88}Sr=0.1194$. Repeated analyses of standards yielded averages of 0.710245±0.000018 (2σ, $n=6$) for Sr standard NIST SRM987, and 0.511870±0.000018 (2σ, $n=6$) for the LaJolla Nd standard. Total chemical blanks were <200 pg for Sr and <100 pg for Nd. Pb isotopic ratios were measured on a VG MM30 mass spectrometer using an optical pyrometer to monitor filament temperature in order to ensure constant fractionation effects. Mass fractionation corrections of 0.09 (±0.03, 2σ)% a.m.u. and 0.24% a.m.u. were applied to Pb isotopic ratios (based on repeated measurements of NIST SRM 981 Pb standard) using Faraday and Daly analogue detectors, respectively. Total procedural blanks are ≤100 pg.

5. Re–Os and Sr, Nd and Pb isotope results

5.1. Re–Os isotope results

The Lijiang basalts have low Os concentrations (0.08–0.49 ppb) and high Re/Os ratios (0.08–1.78). In contrast, with the exception of one sample (DJ03-39), the Lijiang picrites have high Os contents (1.5–2.3 parts per billion (ppb)) and unusually low Re contents (<0.07 ppb). The Re/Os ratios (<0.07) are similar to those observed in mantle xenoliths, but different from picrites from other areas; e.g., Hawaii (Brandon et al., 1999), East Greenland (Brooks et al., 1999) and Karoo (Ellam et al., 1992) and Gorgona komatiites (Brandon et al., 2003) (Fig. 3a,b and Table 1). The Lijiang picrites extend to higher Os concentrations (up to 2.33 ppb) and lower Re/Os ratios (<0.02) in

Table 1
Os isotopic compositions of the Lijiang picrites and associated basalts

Sample No.	Lithology	Re (ppb)	Os (ppb)	$^{187}Re/^{188}Os$	$^{187}Os/^{188}Os^a$	± 2σ	$^{187}Os/^{188}Os^b$	γOs^c	MgO (wt.%)	TiO_2 (wt.%)	Ti/Y	Yb (ppm)	Ni (ppm)	$(La/Yb)_n$
DJ-34	PB	0.086	0.164	2.4765	0.1419	0.0008	0.1312	4.2	11.92	2.16	594	1.86	241	6.63
DJ-33	PB	0.057	0.361	0.7407	0.1338	0.0002	0.1306	3.8	10.74	2.26	630	1.81	259	6.36
DJ-20	AB	0.712	0.491	6.8483	0.1577	0.0005	0.1281	1.8	8.61	3.16	684	1.68	126	10.63
DJ-14	PB	0.020	0.246	0.3840	0.1341	0.0005	0.1324	5.2	10.16	1.99	557	1.81	174	8.32
DJ-1	AB	0.148	0.083	8.5536	0.2551	0.0014	0.2181	73.3	4.17	4.23	722	1.83	45.5	17.26
SM03-4	AB	0.045	0.489	0.4348	0.1413	0.0002	0.1394	10.8	11.59	2.34	678	2.03	394	11.67
DJ03-30	Pic	0.058	2.329	0.1173	0.1233	0.0004	0.1228	−2.4	18.72	1.53	637	1.56	786	11.18
DJ03-39	Pic	0.051	0.320	0.7587	0.1261	0.0002	0.1228	−2.4	19.13	1.83	675	1.40	967	7.33
DJ03-37	Pic	0.014	2.182	0.0308	0.1247	0.0001	0.1246	−1.0	26.69	1.06	697	1.01	1336	5.85
DJ03-44	Pic	0.046	2.163	0.0998	0.1241	0.0001	0.1237	−1.7	13.70	1.86	653	1.87	715	5.81
DJ-31	Pic	0.036	2.640	0.0646	0.1250	0.0002	0.1247	−0.9	26.82	1.14	625	0.91	1272	5.38
DJ03-45	Pic	0.049	2.129	0.1082	0.1258	0.0001	0.1253	−0.4	27.05	1.44	654	1.05	1147	7.20
DJ03-46	Pic	0.029	1.631	0.0840	0.1242	0.0003	0.1238	−1.6	16.00	2.06	922	1.54	734	11.84
DJ03-35	Pic	0.049	2.217	0.1044	0.1242	0.0002	0.1237	−1.7	20.87	1.86	648	1.46	948	11.88
DJ03-35-1	Pic	0.047	2.268	0.0977	0.1241	0.0002	0.1237	−1.7	20.83	1.87	648	1.48	940	11.87
DJ03-4	Pic	0.065	2.235	0.1381	0.1240	0.0002	0.1234	−1.9	18.88	1.73	656	1.63	922	6.16
SM03-6	Pic	0.196	2.299	0.4030	0.1266	0.0001	0.1249	−0.8	22.4	1.73	609	1.34	945	7.19
SM03-1	Pic	0.058	2.051	0.1341	0.1247	0.0001	0.1241	−1.4	19.21	1.72	607	1.71	976	6.21

Pic-picrite; PB-pyroxene-phyric basalt; AB-aphyric basalt. [a]Present day $^{187}Os/^{188}Os$. [b]Age corrected $^{187}Os/^{188}Os$ ratios at 259 Ma using $\lambda=1.666\times10^{-11}$ yr^{-1} (Smoliar et al., 1996). [c]Age corrected γOs values. γOs is the percentage difference between the age-corrected $^{187}Os/^{188}Os$ ratio and the age-corrected $^{187}Os/^{188}Os$ ratio of a chondritic mantle where the present day chondritic mantle has $^{187}Os/^{188}Os=0.12757$ and $^{187}Re/^{188}Os=0.3972$ (Walker et al., 1989).

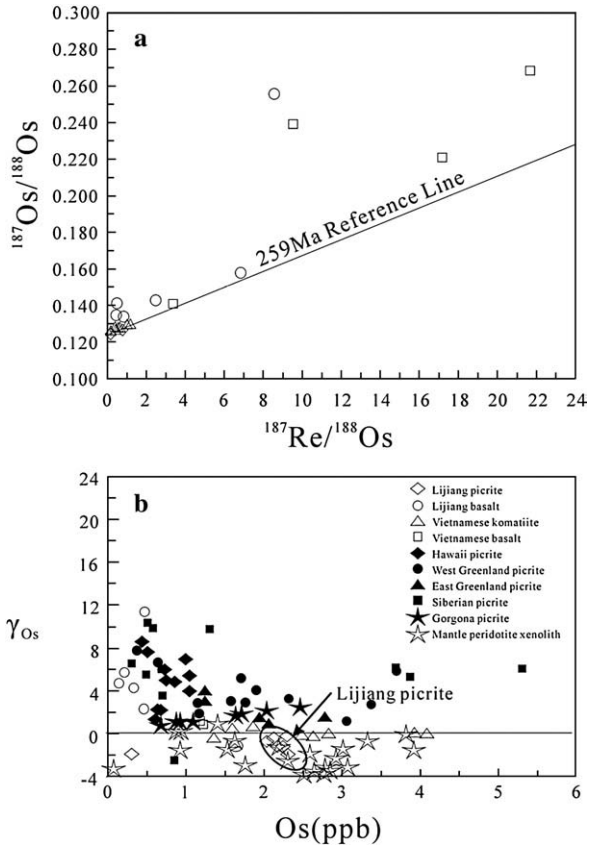

Fig. 4. (a) $^{187}Os/^{188}Os$ vs. $^{187}Re/^{188}Os$ diagrams of picrites and basalts. The Vietnamese komatiites and basalts are also plotted. The Lijiang picrites and Vietnamese komatiites plotted close to the 259 Ma Reference Line, while the basalts have higher $^{187}Os/^{188}Os$ ratios, which can be attributed to crustal contamination. (b) $\gamma_{Os}(t)$ vs. Os diagram. Data sources: Vietnamese komatiites and basalts (Hanski et al., 2004); Hawaiian picrites (Brandon et al., 1999); West Greenland picrites (Schaefer et al., 2000); East Greenland picrites (Brooks et al., 1999); Siberian Traps picrites (Horan et al., 1995); Gorgona komatiites (Brandon et al., 2003); mantle peridotite xenoliths (Pearson et al., 1995; Ionov et al., 2006; Bizimis et al., 2007). Sample DJ-1 is not shown because of its very high $\gamma_{Os}(t)$ value (73.3).

comparison with picrites from many other CFBs and oceanic islands that are considered to be related to mantle plumes, but similar to those from Curaçao (Walker et al., 1999). This is unusual in picritic lavas (Fig. 3b). Komatiites from northern Vietnam, which were considered to be a part of the Emeishan FBP (Hanski et al., 2004), have similar Os concentrations to the Lijiang picrites, but much more variable Re concentrations (Fig. 3a). In contrast, basalts from Vietnam have lower Os concentrations, but much higher Re/Os ratios than komatiites (Fig. 3b).

Initial Os isotopic ratios are usually described in terms of $\gamma_{Os}(t)$, the percent deviation in $^{187}Os/^{188}Os$ of a sample at a given time, from that of the average for carbonaceous chondrites (Walker et al., 1994). The Lijiang picrites from the two sections have similar initial Os isotopic compositions, both with negative $\gamma_{Os}(t)$ values (t=259 Ma) that range from −0.4 to −2.4 and $^{187}Re/^{188}Os$ ratios that range from 0.031 to 0.759 (Table 1). Together, they form a very tight cluster on plots involving these ratios (Table 1, Fig. 4a). The $\gamma_{Os}(t)$ values of the Lijiang picrites are slightly lower than Vietnamese komatiites (0.6 to −0.5), and are generally much lower than those from some other CFBs and ocean island picrites, e.g., Siberian Traps (3.4 to 10.2, Horan et al., 1995), Hawaii (1.39 to 6.69, Brandon et al., 1999), East and West Greenland (0.65 to 6.5, Brooks et al., 1999; Schaefer et al., 2000), and Karoo (0.2 to 12.1, Ellam et al., 1992), but similar to komatiites and picrites from Gorgona and Curaçao (Walker et al., 1999) and Baffin (Kent et al., 2004). They are, however, much higher than many mantle peridotite xenoliths (Fig. 4b). In contrast, the Lijiang basalts have much higher $\gamma_{Os}(t)$ values that vary from 1.8 and 10.8 for five of the analysed samples, and extend up to 73.3 in one sample.

5.2. Sr, Nd and Pb isotope results

The Lijiang picrites and basalts define a relatively small range of $\varepsilon_{Nd}(t)$ values (t=259 Ma) from +4.0 to −1.3 (Table 2; Fig. 5). There is no significant difference between picritic and basaltic samples, +3.0 to −1.3 for basalts and +4.0 to −0.6 for picrites. Values of $(^{87}Sr/^{86}Sr)_t$ vary from 0.70344 to 0.70523. This range is notably smaller than those for many other continental flood basalts, including the Karoo, Deccan Traps, Columbia River, Paraná, and Siberian Traps, although it is larger than found for the intra-oceanic Caribbean or Ontong Java plateau (see Hawkesworth et al., 1984; Carlson and Hart, 1988; Mahoney, 1988; Kerr et al., 1997; Peate, 1997; Sharma, 1997; Tejada et al., 2004, and references therein).

The range of age-corrected Pb isotope ratios is also relatively small compared with those of other continental flood basalts: $(^{206}Pb/^{204}Pb)_t$ varies from 17.60 to 18.73, $(^{207}Pb/^{204}Pb)_t$ from 15.50 to 15.68, and $(^{208}Pb/^{204}Pb)_t$ from 38.02 to 39.20. The data are broadly similar in this respect to Indian Ocean hotspot and ridge basalts.

Table 2
Sr, Nd and Pb isotopic compositions of the Lijiang picrites and associated basalts

Sample No.	$(^{143}Nd/^{144}Nd)_o$	$(^{87}Sr/^{86}Sr)_o$	$(^{206}Pb/^{204}Pb)_o$	$(^{207}Pb/^{204}Pb)_o$	$(^{208}Pb/^{204}Pb)_o$	Nd, ppm	Sm ppm	Sr ppm	Rb ppm	Pb ppm	U ppm	Th ppm	$(^{143}Nd/^{144}Nd)_t$	ε_{Nd} (t)	$(^{87}Sr/^{86}Sr)_t$	$(^{206}Pb/^{204}Pb)_t$	$(^{207}Pb/^{204}Pb)_t$	$(^{208}Pb/^{204}Pb)_t$
DJ-34	0.512698	0.70495	19.158	15.603	39.256	21.11	4.800	290.1	14.2	3.24	0.46	1.70	0.512473	3.0	0.70445	18.734	15.586	38.969
DJ-33	0.512717	0.70664	18.979	15.608	39.062	21.23	4.923	194.4	55.0	5.99	0.48	2.18	0.512488	3.4	0.70379	18.742	15.598	38.851
DJ-20	0.512681	0.70513	18.703	15.570	39.233	30.18	6.723	423.7	22.8	2.12	0.15	1.43	0.512461	2.8	0.70458	18.493	15.562	38.876
DJ-14	0.512494	0.70534	18.792	15.605	39.292	19.35	4.703	2109	21.5	2.52	0.67	3.44	0.512254	−1.3	0.70523	18.002	15.573	38.553
DJ-1	0.512558	0.70701	18.825	15.603	39.518	58.55	12.26	228.0	47.6	2.45	0.50	3.19	0.512351	0.7	0.704906	18.218	15.579	38.813
SM03-4	0.512537	0.70540	19.061	15.612	39.593	34.17	6.813	142.5	4.70	2.75	0.98	4.29	0.512340	0.5	0.705063	17.997	15.569	38.731
DJ03-30	0.512472	0.70625	18.075	15.514	38.351	22.45	4.257	49.83	6.19	3.95	0.65	2.41	0.512285	−0.6	0.704996	17.599	15.495	38.017
DJ03-39	0.512683	0.70532	18.636	15.551	38.883	22.64	4.998	142.7	14.6	3.17	0.41	1.83	0.512464	2.9	0.704284	18.258	15.536	38.570
DJ03-37	0.512690	0.70506	18.611	15.572	38.874	11.50	2.714	32.35	0.53	1.37	0.22	1.01	0.512456	2.7	0.704893	18.139	15.554	38.494
DJ03-44	0.512678	0.704843	18.748	15.563	39.428	4.66	20.120	74.37	4.61	1.10	0.30	2.14	0.512449	2.6	0.70422	17.940	15.532	38.416
DJ-31	0.512773	0.70515				9.56	2.400	28.75	4.80	2.08	0.24	0.81	0.512524	4.0	0.70344			
DJ03-45	0.512710	0.70480	18.830	15.563	39.025	12.49	2.861	82.82	11.5	2.21	0.28	1.26	0.512483	3.3	0.703399	18.460	15.549	38.724
DJ03-46	0.512544	0.70522	18.763	15.557	39.193	26.21	5.194	25.38	0.66	2.52	0.77	3.62	0.512348	0.6	0.704962	17.860	15.521	38.415
DJ03-35	0.512714	0.70578	18.395	15.544	38.767	19.66	4.550	122.7	16.3	5.98	0.40	2.90	0.512485	3.3	0.704444	18.199	15.535	38.487
DJ03-35–1	0.512502	0.70575	18.393	15.575	38.782	21.95	4.262	136.2	17.8	6.01	0.41	3.02	0.512310	−0.1	0.704433	18.193	15.567	38.493
DJ03-4	0.512733	0.70472	19.160	15.609	39.443	19.28	4.451	174.9	4.94	1.19	0.40	1.55	0.512504	3.7	0.704437	18.157	15.570	38.762
SM03-6	0.512714	0.70463	19.160	15.702	39.599	16.49	3.800	152.2	6.86	3.05	0.65	1.97	0.512464	2.9	0.704172	18.524	15.676	39.242
SM03-1	0.512692	0.70456	19.217	15.594	39.463	19.66	4.550	174.8	4.12	1.44	0.36	1.74	0.512485	3.3	0.704351	18.470	15.565	38.827

Measured isotopic ratios (subscript) are age-corrected (t) to 259 Ma. Concentrations of Rb, Sr, Sm and Nd are determined by isotope dilution, and U, Th and Pb data are determined by ICP-MS.

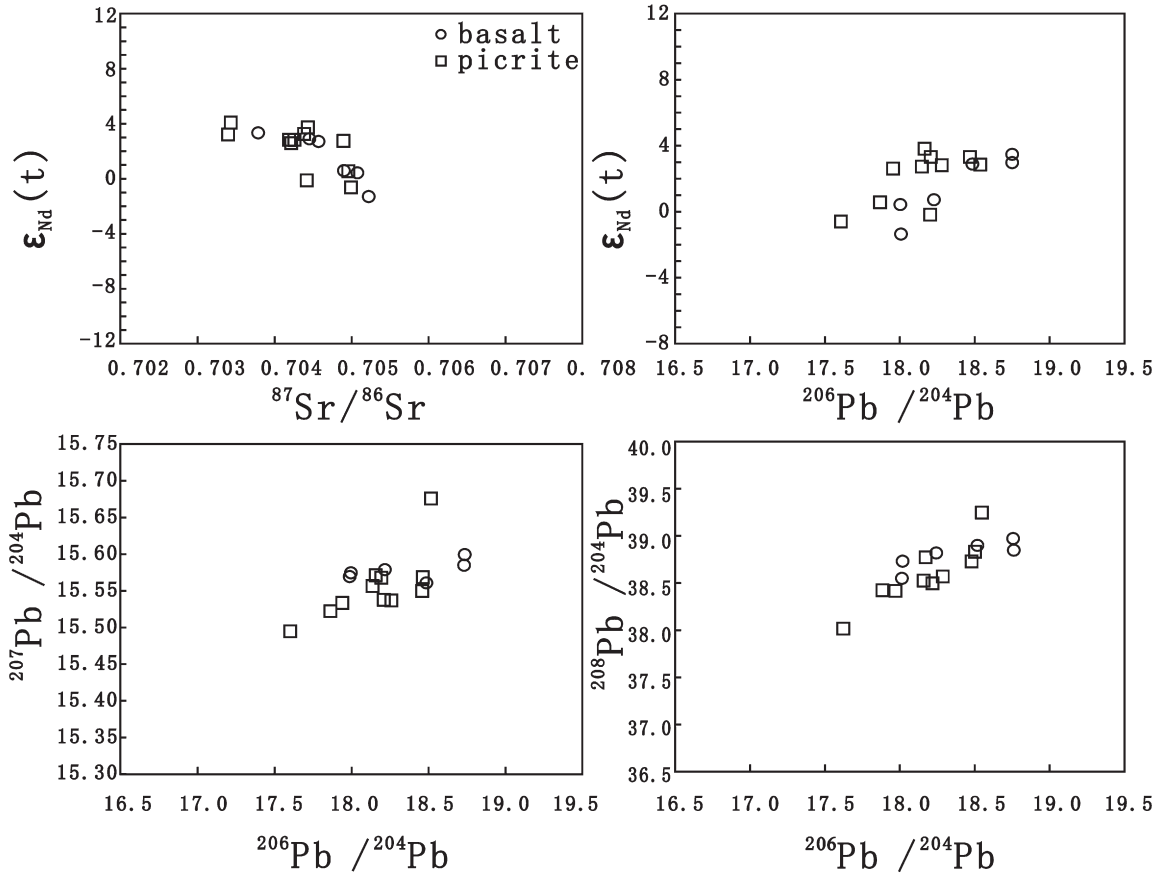

Fig. 5. $\varepsilon_{Nd}(t)$ vs. $(^{87}Sr/^{86}Sr)_t$, $(^{206}Pb/^{204}Pb)_t$, $(^{206}Pb/^{204}Pb)_t$ vs. $(^{207}Pb/^{204}Pb)_t$ and $(^{208}Pb/^{204}Pb)_t$ for the Emeishan basalt and picrite lavas.

It is noted that sample (DJ-1) with the highest $\gamma_{Os}(t)$ value has the lowest Os concentration (0.083 ppb) and a relatively high $(^{87}Sr/^{86}Sr)_t$ ratio (0.704906) and $(^{208}Pb/^{204}Pb)_t$ ratio (38.813, Table 2).

6. Discussion

6.1. Assessment of contribution of a lithospheric mantle component and continental crust

Continental flood basalts (CFB) and oceanic island basalts (OIB) are commonly thought to represent melting products of mantle plumes (e.g., Richards, et al.,1989; Hill, 1991). The Emeishan province of southwestern China is one of three continental flood basalt provinces that formed near the end of the Permian in widely separated locations, the other being the Siberian Traps (Sharma, 1997) and Panjal Traps of northwestern India (e.g. Bhat et al., 1981). The Emeishan province has been the focus of several recent stratigraphic, geochronological, geochemical, and geophysical studies. Evidence for high-temperature magmas and >1 km of doming of the regional lithosphere shortly before volcanism has been documented, and together with associated variations in crustal thickness, upper-mantle and lower-crustal seismic characteristics, and basalt composition, has been argued to strongly support a plume origin (He et al., 2003; Xu et al., 2004; Zhang et al., 2006a, b). However, considerable discussion surrounds the extent of contribution of subcontinental lithospheric mantle (SCLM) and continental crust or recycled crustal materials (e.g., Song et al., 2001; Xiao et al., 2004).

Like other CFBs, the Emeishan flood basalts have been subdivided into low- and high-Ti types (e.g., Xu et al., 2001; Zhang and Wang, 2002; Xiao et al., 2004). Based on a geochemical study of the basaltic rocks from the Binchuan and Yongsheng regions in the western part of the province, Xu et al. (2001) and Xiao et al. (2004) proposed that the low-Ti lavas reflect a greater role for melting at shallower depths in the spinel stability field in the plume axis region, whereas the high-Ti lavas resulted from lower degrees of melting of the mantle at the plume periphery, due to lower temperature and thicker lithosphere. In contrast, on the basis of Os isotopic data for basalts from several localities, Xu et al. (2007) proposed that the low-Ti basalts with radiogenic Os ($\gamma_{Os}(t)$~6.5) have a plume-derived origin, whereas high-Ti basalts with unradiogenic Os isotopic signatures ($\gamma_{Os}(t)$ values range from −0.8 to −1.4) suggest a SCLM component. The range of the Os isotopic data presented in Xu et al. (2007) is in fact much larger with high-Ti basalts providing $\gamma_{Os}(t)$ values between −1.1 and 813, and low-Ti basalts from 6.5 to 332; there is also a large overlap between the high-Ti and low-Ti groups. Our new data for the basaltic rocks overlap with their results (both high- and low-Ti basalts).

Based on the petrography, and major and trace element compositions of the picrites and associated basalts, Zhang et al. (2006a) suggested that the Lijiang basalts were generated from picritic magmas, by crystal fractionation dominated by olivine with minor clinopyroxene and Cr-spinel. However, crystallization alone cannot account for the difference in Os (and other) isotope composition between basalt and picrite. This suggests that during the formation of the basalts, the melts were contaminated with lithospheric material (crust or SCLM).

Previous studies have shown (Esser and Turekian, 1988, Frick et al., 1996) that both ancient upper and lower crust can be significantly enriched in radiogenic Os, although Os isotopic compositions are quite variable in Earth's crust. Estimates of γ_{Os} in the modern upper crust and lower crust are +1230 (Esser and Turekian, 1988) and +1700 to 22000 (Frick et al., 1996), respectively. Hence, γ_{Os} values of the Earth's crust have much higher positive values compared with mantle-derived magmas. The addition of very modest quantities (10%) of crustal materials to plume basalts on ascent through continental crust

would therefore be expected to impart positive γ_{Os} values to the magmas. This is also supported by two simple mixing results for Sr, Nd, and Os isotopic compositions (Fig. 6). In Fig. 6, the addition of very modest quantities of crustal materials to low Os basaltic melts (curve 1) would cause much higher γ_{Os} values than to high-Os picritic melts (curve 2). As indicated in Fig. 6, the Lijiang basalts cannot be modeled solely by contamination of picritic or basaltic melts by crustal materials. It is likely that the basalts were formed by assimilation and fractional crystallization (AFC) processes of picritic magmas (Fig. 6). Hence, high-γ_{Os} basalts resulted from crustal contamination.

For the high-Os picrites, the modeling results imply that their γ_{Os} values, unlike Nd, Sr and Pb isotopes, are little affected by crustal contamination. In Fig. 6, the Lijiang picrites were produced by parental picritic melts contaminated by <16% crustal materials. We caution that the mixing arguments are very model dependent, because the positions of the curves in Fig. 6 can vary with a different choice of the isotopic compositions of two end-members (crust and parental melts). However, the conclusion that crustal contamination would have been unlikely to significantly affect Os isotopic compositions in the high Os picrites is difficult to avoid.

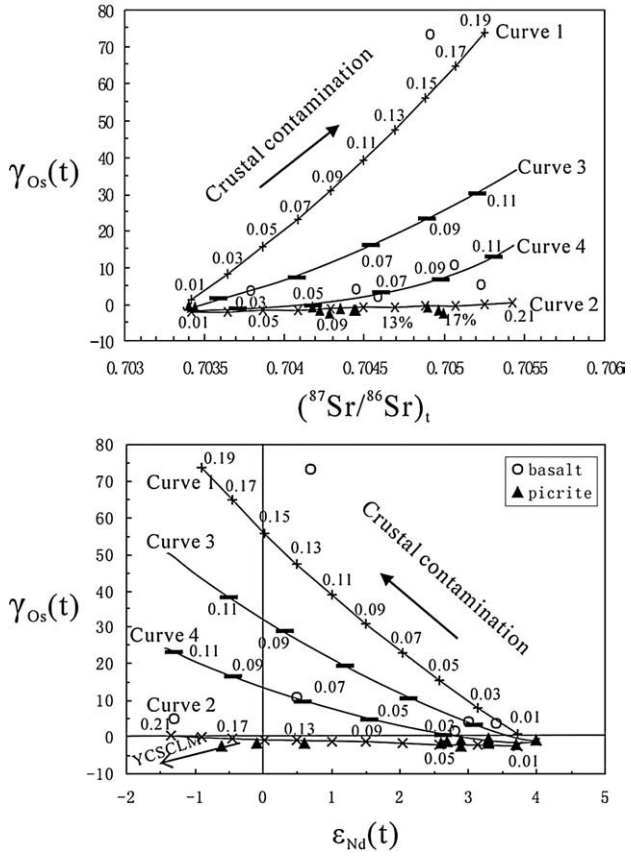

Fig. 6. (a) $(^{87}Sr/^{85}Sr)_t$ vs. $\gamma_{Os}(t)$ and (b) $\varepsilon_{Nd}(t)$ vs. $\gamma_{Os}(t)$ diagrams for the Lijiang picrites and basalts. Curve 1 and curve 2 represent two modeled mixing lines, and Curve 3 and curve 4 represent modeled assimilation and fractional crystallization (AFC) lines, assuming R [(rate of assimilation of crust)/(rate of fractional crystallization)]=8 and 4 respectively. Curve 1 shows mixing between uncontaminated basaltic melt and putative continental crust from the Yangtze craton, and curve 2 shows mixing between picritic melt and continental crust. The $^{187}Os/^{188}Os$(259 Ma) values and Os contents for the presumed Lijiang parental picritic magmas are 0.1228 and 2 ppb, respectively; 0.1228 and 0.06 ppb for uncontaminated basaltic magma, and 1.700 (Esser and Turekian, 1988), and 0.02 ppb (Wang, 2001) for average continental crust. Sr and Nd isotopic data for crust in the Yangtze craton (259 Ma) are from Wang et al. (2006) and Li et al. (2001), and Sr and Nd concentrations are from Yan et al. (1997). Partition coefficient for Os is calculated for olivine+sulphide fractionation assuming $K_{d\ Os}$ olivine/melt=7 (between olivine and melt), $K_{d\ Os}$ sulphide/melt=15,000 (between sulphide and melt) (after McBride et al., 2001). Partition coefficients for Sr and Nd between olivine, clinopyroxene and silicate melt are from Adam and Green (1994). YCSCLM: sublithospheric mantle beneath Yangtze craton (Zhi and Qin, 2004); Modeling shows that curve 2 is consistent with the observed Os isotopic variations of the Lijiang picrites. In contrast, the observed Os isotopic variation of the basalts is consistent with the AFC process rather than a simple mixing model.

6.2. Were the Lijiang picrites sourced from recycled oceanic crust or the SCLM?

Based on measurements of the partitioning of Re between garnet and silicate liquid, Righter and Hauri (1998) proposed that within the stability field of garnet (90 to 100 km), Re could be retained during dehydration or melting of the slab, and thus garnet may play a role in generating high Re/Os ratios (and, over time, high Os isotope ratios) of slab material during subduction zone processing. Elevated Os isotopes should thus be a sensitive indicator of recycled oceanic material, as indicated by Os isotope data for ancient pyroxenites and eclogites (Pearson et al., 1995). Hence, it is unlikely that the Lijiang picrites with unradiogenic Os isotopic compositions are sourced from recycled oceanic crust.

Ancient SCLM, however, generally has sub-chondritic Os isotopic compositions, with γ_{Os} values as low as −20 in the most refractory (harzburgitic) SCLM of Archaean cratons (Walker et. al., 1989; Pearson et al., 1995). This has been attributed to episodes of previous melt extraction. We cannot entirely rule out involvement of the SCLM in the formation of the Emeishan picrites, because we have no information about the composition of the SCLM directly under the study area. However, Re–Os isotopic data for harzburgitic mantle from Nushan (Anhui province) and Panshishan (Jiangsu province) in the Yangtze craton, east of our study area, suggest that refractory portions of the SCLM underlying the Emeishan CFB have strongly negative γ_{Os}, with γ_{Os} (t=259 Ma) values as low as −10. These are likely to be regions of ancient melt depletion, with Re-depletion model ages of 0.5 to 2.0 Ga (Zhi and Qin, 2004). In addition, because SCLM has generally high Os concentrations and low $^{187}Os/^{188}Os$ ratios, a negative co-variation between Os concentrations and $^{187}Os/^{188}Os$ ratios would be expected if interaction with SCLM is significant. As in Fig. 4b, such negative co-variation has not been observed. This strengthens the view that there is little evidence for any significant participation of SCLM in the genesis of the Lijiang picrites. If we assume that the most radiogenic picrite included in this study (γ_{Os}=−0.4) represents the Os isotopic composition of the starting mantle plume prior to SCLM contamination, then the decrease in γ_{Os} value to −2.4 in our Os picrite data set can represent only minimal amounts of SCLM contamination. Two-component mixing calculations suggest that ~14% SCLM contamination can account for the entire range in Os isotopic composition of our picrites, assuming a Emeishan SCLM with 3.4 ppb and a γ_{Os} of −10 (Zhi and Qin, 2004), and picritic melt composition with 2.1 ppb Os and a γ_{Os} of −0.4. However, if we assume the picrite has the average Os isotopic composition of the magmas contaminated by SCLM, then this range in Os isotopic composition can be accounted for by as little as 6% SCLM contamination. On the other hand, distinguishing near chondritic components from mixing with unradiogenic lithosphere reservoirs solely on the basis of Os isotopes could be problematic. Except for two samples (DJ03-30 and DJ03-35-1), all of Lijiang picritic samples have positive $\varepsilon_{Nd}(t)$ values (Table 2). This implies that the contribution of SCLM to the formation of the Lijiang picrites was comparatively minor because the subcontinental lithospheric mantle beneath the Yangtze craton region has negative $\varepsilon_{Nd}(t)$ values (~−20, Qiu et al., 2000). Hence, high-Os picrites represent the best samples of plume mantle tracers (Shirey, 1997). On this basis, the Emeishan mantle plume was relatively depleted in radiogenic Os (γ_{Os} <0).

6.3. Constraints on mantle melting

Rhenium is generally assumed to be much less compatible than Os during melting of mantle peridotite, i.e., Os is a compatible element

whereas Re is a moderately incompatible element (Righter and Hauri, 1998; Burton et al., 2000, 2002; Mallman and O'Neill, 2007; Fonseca et al., 2007). Decreasing degrees of partial melting of mantle should therefore lead to elevated Re/Os ratios in magmas. High $(La/Yb)_n$ ratios (subscript n represents chondrite normalization) can also be ascribed to low partial melting, especially if garnet is residual in the mantle source. However, whilst $(La/Yb)_n$ ratios will not be significantly affected by low-pressure crystal fractionation, Re/Os ratios may increase because of different partition coefficients in olivine, clinopyroxene and Cr-spinel (Burton et al., 2000, 2002). Although segregation of sulfides also leads to elevated Re/Os ratios because Os is much more compatible than Re in sulfide (Burton et al., 2002), the role of sulfides should be negligible, given very low contents of sulfides in the picrites (no sulfides have been separated from about 20 kg picrite samples by heavy liquid techniques, Zhang et al., 2006b). The very low Re contents of the picrites could be attributed to high initial melt temperature (1630–1690 °C, Zhang et al., 2006a), because the partition coefficient of Re reduces with increasing temperature (Fonseca et al., 2007).

As indicated in Fig. 7, there are two groups of picrites and basalts with different $(La/Yb)_n$ ratios, which do not appear to be related to Ti/Y. We suggest that those picrites with higher $(La/Yb)_n$ ratios were produced by lower degree of melting, and the basalts with higher $(La/Yb)_n$ ratios were formed by crystal fractionation of these picritic magmas. Conversely, the basalts with lower $(La/Yb)_n$ ratios were derived from the picritic magmas with similarly low $(La/Yb)_n$ ratios that resulted from relatively higher degree of melting of mantle peridotite. One sample (DJ-1) with the highest $(La/Yb)_n$ and Re/Os ratios could be ascribed to the AFC processes (Fig. 6).

Unfortunately, there are no partition coefficient data for Re and Os in mantle minerals, making it impossible to quantitatively estimate the degree of partial melting via Re and Os data. If we assume unmelted peridotite to be a near-primary mantle, 2 to 7% partial melting of such mantle will account for the magmas with $(La/Yb)_n$ ratios of 3 to 11.7. Although the modeled $(La/Yb)_n$ ratios will vary with a different choice of melting model, distribution coefficients, source composition, and/or mineral proportions, the Lijiang picritic magmas were formed by small degrees of partial melting (Zhang et al., 2006a). Experimental work has suggested that picrites can be produced by small degrees of partial melting under high pressure conditions (Herzberg and O'Hara, 1998; Herzberg and Zhang, 1996). Zhang et al. (2006a) proposed that the Lijiang picrites were generated under high pressure (ca. 4 GPa). Hence, the Lijiang picrites could result from small degrees of partial melting under high pressure conditions.

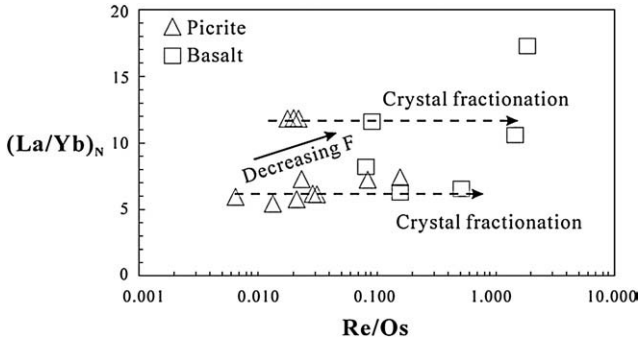

Fig. 7. Re/Os-$(La/Yb)_n$ diagram. *F* represents degree of melting. Based on $(La/Yb)_n$ ratios, the Lijiang picrites and basalts except for one sample (DJ-1) can be divided into two groups, which can be generated by the differentiation of two different parental magmas that were produced by different degrees of melting: the higher $(La/Yb)_n$ ratios, the lower degree of melting. The fractional crystallization leads to similar $(La/Yb)_n$ ratios, but elevated Re/Os ratios. One sample (DJ-1) with the highest $(La/Yb)_n$ and Re/Os ratios could be ascribed to crustal contamination, which gives rise to elevated $(La/Yb)_n$ and Re/Os ratios.

6.4. Constraints on the nature of the Emeishan mantle plume

Although some researchers proposed that the Emeishan CFB might have been derived from a plume originating at the CMB, similar to the case for the Siberian CFB (Horan et al., 1995; Lo et al., 2002; Wang, 2001), there is no evidence to support this assumption. The Re–Os isotopic system is a potentially powerful tool for constraining the depths of origin of mantle plumes (Walker et al., 1995, 1997).

As described above, all Lijiang picrites have relatively low $\gamma_{Os}(t)$ values (<0). A low Os isotopic component is unusual compared to OIB-related picrites and basalts, e.g., Azores (Widom and Shirey, 1996), Canary Islands (Widom et al., 1999), Samoa (Hauri and Hart, 1993), Siberian Traps (Horan et al., 1995), East Greenland (Brooks et al., 1999), West Greenland (Schaefer et al., 2000) and Hawaii (Hauri et al., 1996; Lassiter and Hauri, 1998; Brandon et al., 1999), have positive $\gamma_{Os}(t)$ values (Fig. 4b). However, the low Os isotopic component is also recognized in some komatiites and picrites, e.g., Gorgona and Curaçao (Walker et al., 1999) and Baffin (Kent et al., 2004). Anderson (2004) proposed that these putative plume-derived rocks were sourced in the asthenospheric mantle. However, the combination of hotspot-type geochemical characteristics with the evidence for a high mantle-source temperature (Zhang et al., 2006a) and the apparently very strong evidence for a large amount of regional lithospheric uplift immediately preceding flood volcanism (He et al., 2003; Xu et al., 2004) appears consistent with some type of mantle upwelling origin for the Emeishan large igneous province. Thus, this raises important question: Is the mantle plume-derived from core–mantle boundary or upper–lower mantle boundary? As stated above, the Lijiang picrites have no signature of any enrichment of ^{187}Os. Consequently, our new Os isotopic data do not require any direct involvement of the core in the formation of Emeishan CFB. Another possibility is that the Emeishan plume is also derived from parts of the D″ layer which have low γ_{Os}; in other words, the D″ layer is compositionally heterogeneous. However, at present there is no such evidence to support this assumption. Alternately, it is possible that the Emeishan mantle plume originated from the upper–lower mantle boundary.

7. Conclusions

The Lijiang picrites offer a rare opportunity to evaluate the nature of primary plume isotopic compositions in a voluminous CFB province. They are characterised by high Os abundances (~2 ppb), and relatively low Os isotopes ($\gamma_{Os}(t)<0$) for plume-related magmas. By contrast, the associated basalts have low Os concentrations (0.08–0.49 ppb) and suprachondritic Os isotope compositions with $\gamma_{Os}(t)$ (1.8–73.3), which overlap those of the basalts from other localities in the province, and could be attributed to low extent of crustal contamination. The lower $\gamma_{Os}(t)$ values of the Lijiang picrites relative to global plume-related picrites, did not result from a significant degree of interaction of the picrites with ancient subcontinental lithospheric mantle, but are the initial mantle plume isotopic signature, and therefore suggest that the mantle source of the Emeishan picrites did not equilibrate with Earth's core at the CMB or contain recycled crustal components. This implies that the Emeishan mantle plume may have originated from the 670 km discontinuity between the upper and lower mantle.

Acknowledgements

We are grateful to Xie Zhi, Gao Jianfeng and Yang Tao for assistance with the work. We thank reviewers Richard J. Walker and Chris Dale for their thoughtful and constructive comments. The editorial suggestions of Richard W. Carlson helped to improve the revised version. The study was supported by the National Natural Science Foundation of China (Grant No. 40473008 and 40572036 to XCZ, 40273020 to ZCZ,), Program for New Century Excellent Talents in University (Grant No. NCET-04-0728), 111 Project (B07011) and PCSIRT. Finally, XCZ thanks

specially Dr. Reisberg at CRPG, CNRS, France, for her suggestions and helps during our Re–Os isotope lab works in USTC.

References

Adam, J., Green, T.H., 1994. The effects of pressure and temperature on the partitioning of Ti, Sr and REE between amphibole, clinopyroxene and basanitic melts. Chem. Geol 117, 219–234.

Allègre, C.H., Turcotte, D.L., 1985. Geodynamic mixing in the mesosphere boundary layer and the origin of oceanic islands. Geophys. Res. Lett 97, 10997–11009.

Anderson, D.L., 2004. The statistics and distribution of helium in the mantle. Inter. Geol. Rev 42, 289–311.

Arndt, N.T., Czamanske, G.K., Wooden, J.L., Fedorenko, V.A., 1993. Mantle and crustal contributions to continental flood basalt volcanism. Tectonophysics 223, 39–52.

Bennett, V.C., Norman, M.D., Garcia, M.O., 2000. Rhenium and platinum group element abundances correlated with mantle source components in Hawaiian picrites: sulphides in the plume. Earth Planet. Sci. Lett 183, 513–526.

Bhat, I., Zainuddin, S.M., Rais, A., 1981. The Panjal Trap chemistry and the birth of Tethys. Geol. Mag 118, 355–365.

Bijwaard, H., Spakman, W., 1999. Tomographic evidence for a narrow whole mantle plume below Iceland. Earth Planet. Sci. Lett 166, 121–126.

Birck, J.L., Barman, M.R., Capmas, F., 1997. Re–Os isotopic measurements at the femtomole level in natural samples. Geostand Newsl 21, 19–27.

Bizimis, M., Griselin, M., Lassiter, J.C., Salters, V.J.M., Sen, G., 2007. Ancient recycled mantle lithosphere in the Hawaiian plume: Osmium–Hafnium isotopic evidence from peridotite mantle xenoliths. Earth Planet. Sci. Lett 257, 259–273.

Boven, A., Pasteels, P., Punzalan, L.E., Liu, J., Luo, X., Zhang, W., Guo, Z., Hertogen, J., 2002. $^{40}Ar/^{39}Ar$ geochronological constraints on the age and evolution of the Permo-Triassic Emeishan volcanic province, southwest China. J. Asian Earth Sci 20, 157–175.

Brandon, A.D., Norman, M.D., Walker, R.J., Morgan, J.W., 1999. $^{186}Os–^{187}Os$ systematics of Hawaiian picrites. Earth Planet. Sci. Lett 174, 25–42.

Brandon, A.D., Walker, R.J., Morgan, J.W., Norman, M.D., Prichard, H.M., 1998. Coupled ^{186}Os and ^{187}Os evidence for core–mantle interaction. Science 280, 1570–1573.

Brandon, A.D., Walker, R.J., Puchtel, I.S., Bechker, H., Humayun, M., Revillon, S., 2003. $^{186}Os–^{187}Os$ systematics of Gorgona Island komatiites: implications for early growth of the inner core. Earth Planet. Sci. Lett 206, 411–426.

Brooks, C.K., Keays, R.R., Lambert, D.D., Frick, L.D., Nielsen, T.F.D., 1999. Re–Os isotope geochemistry of Tertiary picritic and basaltic magmatism of East Greenland: constraints on plume-lithosphere interactions and the genesis of the Platinova reef, Skaergaard intrusion. Lithos 47, 107–126.

Burton, K.W., Gannoun, A., Birck, J.L., Allègre, C.J., Schiano, P., Clocchiatti, R., Alard, O., 2002. The compatibility of rhenium and osmium in natural olivine and their behaviour during mantle melting and basalt genesis. Earth Planet. Sci. Lett 198, 63–76.

Burton, K.W., Schiano, P., Birck, J.L., Allègre, C.J., Rehkämper, M., Halli-day, A.N., Dawson, J.B., 2000. The distribution and behaviour of rhenium and osmium amongst mantle minerals and the age of the lithospheric mantle beneath Tanzania. Earth Planet. Sci. Lett 183, 93–106.

Carlson, R.W., Hart, W.K., 1988. Flood basalt volcanism in the northwestern United States. In: Macdougall, J.D. (Ed.), Continental Flood Basalts. Kluwer Academic, Dordrecht, pp. 35–62.

Chung, S.L., Jahn, B.M., 1995. Plume-lithosphere interaction in generation of the Emeishan flood basalts at the Permian-Triassic boundary. Geology 23, 889–892.

Ellam, R.M., Carlson, R.W., Shirey, S.B., 1992. Evidence from Re–Os isotopes for plume-lithosphere mixing in Karoo flood basalt genesis. Nature 359, 718–721.

Enkin, R.J., Courtillot, V., Leloup, P.h., Yang, Z., Xing, L., Zhang, J., Zhuang, Z., 1992. The paleomagnetic record of Uppermost Permian, Lower Triassic rocks from the South China Block. Geophys. Res. Lett 19, 2147–2150.

Esser, B.L., Turekian, K.K., 1988. Accretion rate of extraterrestrial particles determined from osmium isotope systematics of Pacific Pelagic clay and manganese nodules. Geochim. Cosmochim.Acta 52, 1383–1388.

Fonseca, B.O.C., Mallmann, G., O'Neill, H.S.C., Campbell, I.H., 2007. How chalcophile is rhenium? An experimental study of the solubility of Re in sulphide mattes. Earth Planet. Sci. Lett 260, 537–548.

Frick, L.R., Lambert, D.D., Cartwright, I., 1996. Re–Os dating of metamorphism in the Lewisian complex, NW Scotland. Goldschmidt Symposium_Heidelberg. Journal of Conference Abstracts 1, 185.

Gallagher, K., Hawkesworth, C.J., 1992. Dehydration melting and the generation of continental flood basalts. Nature 258, 57–59.

Guo, F., Fan, W.M., Wang, Y.J., Li, C.W., 2004. When did the Emeishan plume activity start? Geochronological evidence from ultramafic–mafic dikes in Southwestern China. Inter, Geol. Rev 46, 226–234.

Hanski, E., Walker, R.J., Huhma, H., Polyakov, G.V., Balykin, P.A., Hoa, T.T., Phuong, N.T., 2004. Origin of Permian-Triassic komatiites, northwestern Vietnam. Contrib. Mineral. Petrol 147, 453–469.

Hauri, E.H., Hart, S.R., 1993. Re–Os systematics of HIMU and EMII oceanic island basalts from the south Pacific Ocean. Earth Planet. Sci. Lett 114, 353–371.

Hauri, E.H., Lassiter, J.C., DePaolo, D.J., 1996. Osmium isotope systematics of drilled lavas from Mauna Loa, Hawaii. J. Geophys. Res 101, 11793–11806.

Hawkesworth, C.J., Marsh, J.S., Duncan, A.R., Erlank, A.J., Norry, M.J., 1984. The role of continental lithosphere in the generation of the Karoo volcanic rocks: evidence from combined Nd- and Sr-isotope studies. In: Erlank, A.J. (Ed.), Petrogenesis of the Volcanic Rocks of the Karoo Province. Spec. Publ, vol. 13. Geol. Soc. South Afr, pp. 341–354.

He, B., Xu, Y., Xiao, L., Chung, S., Wang, Y., 2003. Sedimentary evidence for a rapid, kilometer-scale crustal doming prior to the eruption of the Emeishan flood basalts. Earth Planet. Sci. Lett 213, 391–405.

He, B., Xu, Y.G., Huang, X.L., Luo, Z.Y., Shi, Y.R., Yang, Q.J., Yu, S.Y., 2007. Age and duration of the Emeishan flood volcanism, SW China: Geochemistry and SHRIMP zircon U–Pb dating of silicic ignimbrites, post-volcanic. Earth Planet. Sci. Lett. 255, 306–323.

Helmberger, D.V., Wen, L., Ding, X., 1998. Seismic evidence that the source of the Iceland hotspot lies at the core–mantle boundary. Nature 396, 251–255.

Herzberg, C., O'Hara, M.J., 1998. Phase equilibrium constraints on the origin of basalts, picrites, and komatites. Earth Sci. Rev 44, 39–79.

Herzberg, C., Zhang, J., 1996. Melting experiments on anhydrous peridotite KLB-1: compositions of magmas in the upper mantle and transition zone. J. Geophys. Res 101, 8271–8295.

Hill, R.I., 1991. Starting plumes and continental break-up. Earth Planet. Sci. Lett 104, 398–416.

Hofmann, A.W., 1997. Mantle plumes from ancient oceanic crust. Earth Planet. Sci. Lett 57, 421–436.

Horan, M.F., Walker, R.J., Fedorenko, V.A., Czamanske, G.K., 1995. Osmium and neodymium isotopic constraints on the temporal and spatial evolution of Siberian flood basalt sources. Geochim. Cosmochim. Acta 59, 5159–5168.

Ionov, D.A., Shirey, S.B., Weis, D., Brügmann, G., 2006. Os–Hf–Sr–Nd isotope and PGE systematics of spinel peridotite xenoliths from Tok, SE Siberian craton: Effects of pervasive metasomatism in shallow refractory mantle. Earth Planet. Sci. Lett 241, 47–64.

Kent, A.J.R., Stolper, E.M., Francis, D., Woodhead, J., Frei, R., Eiler, J., 2004. Mantle heterogeneity during the formation of the North Atlantic Igneous Province: Constraints from trace element and Sr–Nd–Os–O isotope systematics of Baffin Island picrites. Geochemistry Geophysics Geosystems 5, Q11004. doi:10.1029/2004GC000743.

Kerr, A.C., Tarney, J., Marriner, G.F., Nivia, A., Saunders, A.D., 1997. The Caribbean–Colombian Cretaceous igneous province: the internal anatomy of an oceanic plateau. In: Mahoney, J.J., Coffin, M.F. (Eds.), Large Igneous Provinces: Continental, Oceanic and Planetary Flood Volcanism. Geophysical Monographs, vol. 100. Amer. Geophys. Uni, pp. 123–144.

Larsen, T.B., Yuen, D.A., 1997. Fast plumeheads: temperature dependent versus non-Newtonian rheology: Geophys. Res. Lett 24, 1995–1998.

Larsen, T.B., Yuen, D.A., Storey, M., 1999. Ultrafast mantle plumes and implications for flood basalt volcanism in the northern Atlantic region. Tectonophysics 311, 31–43.

Lassiter, J.C., Hauri, E.H., 1998. Osmium-isotope variations in Hawaiian lavas: evidence for recycled oceanic lithosphere in the Hawaiian plume. Earth Planet. Sci. Lett 164, 483–496.

Li, L., Zheng, Y.F., Zhou, J.B., 2001. Dynamic model of Pb isotope evolution in the continental crust of China. Acta Petrol. Sin 16, 61–68.

Lo, C., Chung, S., Lee, T., Wu, G., 2002. Age of the Emeishan flood magmatism and relations to Permian-Triassic boundary events. Earth Planet. Sci. Lett 198, 449–458.

Mahoney, J.J., 1988. Deccan Traps. In: Macdougall, J.D. (Ed.), Continental Flood Basalts Kluwe. Academic Publishers, Dordrecht, pp. 151–194.

Mallmann, G., O'Neill, H.S.C., 2007. The effect of oxygen fugacity on the partitioning of rhenium between crystals and silicate melt during mantle melting. Geochim. Cosmochim. Acta 71, 2837–2857.

McBride, J.S., Lambert, D.D., Nicholls, I.A., Price, R.C., 2001. Osmium isotopic evidence for crust–mantle interactionin the genesis of continental intraplate basalts from the Newer volcanics province, Southeastern Australia. J. Petrol 42, 1197–1218.

Montelli, R., Nolet, G., Dahlen, F.A., Masters, G., 2006. A catalogue of deep mantle plumes: New results from finite-frequency tomography. Geochemistry Geophysics Geosystems 7.

Montelli, R., Nolet, G., Dahlen, F.A., Masters, G., Engdahl, E.R., Hung, S.H., 2003. Finite-frequency tomography reveals a variety of plumes in the mantle. Science 303, 338–343.

Nägler, T.F., Frei, R., 1997. Plug in Os distillation. Schweiz Mineral. Petrogr. Mitt 77, 123–127.

Nolet, G., Allen, R., Zhao, D., 2007. Mantle plume tomography. Chem. Geol 241, 248–263.

Nolet, G., Karato, S.I., Montelli, R., 2006. Plume fluxes from seismic tomography. Earth Planet. Sci. Lett 248, 685–699.

Pearson, D.G., Carlson, R.W., Shirey, S.B., Boyd, F.R., Nixon, P.H., 1995. The stabilisation of Archaean lithospheric mantle: a Re–Os isotope study of peridotite xenoliths from the Kaapvaal craton. Earth Planet. Sci. Lett 134, 341–357.

Peate, D.W., 1997. The Paraná–Etendeka province. In: Mahoney, J.J., Coffin, M.F. (Eds.), Large Igneous Provinces: Continental, Oceanic and Planetary Flood Volcanism. Geophys. Uni, vol. 100. Geophysical Monographs, Amer, pp. 217–245.

Qiu, Y.M., Gao, S., McNaughton, N.J., Groves, D.I., Li, W.L., 2000. First evidence of > 3.2 Ga continental crust in the Yangtze craton of south China and its implications for Archean crustal evolution and Phanerozoic tectonics. Geology 28, 11–14.

Reisberg, L., Lorand, J.P., Bedini, R.M., 2004. Reliability of Os model ages in pervasively metasomatized continental mantle lithosphere: A case study of Sidamo spinel peridotite xenoliths (East African Rift, Ethiopia). Chem. Geol 208, 119–140.

Richards, M.A., Duncan, R.A., Courtillot, V.E., 1989. Flood-basalt and hot spot tracks: plume heads and tails. Science 246, 103–107.

Righter, K., Hauri, E.H., 1998. Compatibility of rheniumin garnet during mantle melting and magma genesis. Science 280, 1737–1741.

Russell, S.S., Lay, T., Garnero, E.J., 1998. Seismic evidence for small-scale dynamics in the lowermost mantle at the root of the Hawaiian hotspot. Nature 396, 255–258.

Saunders, A.D., Jones, S.M., Morgan, L.A., Pierce, K.L., Widdowson, M., Xu, Y.G., 2007. Regional uplift associated with continental large igneous provinces: the roles of mantle plumes and the lithosphere. Chem. Geol 241, 282–318.

Schaefer, B.F., Parkinson, I.J., Hawkesworth, C.J., 2000. Deep mantle plume osmium isotope signature from West Greenland Tertiary picrites. Earth Planet. Sci. Lett 175, 105–118.
Sharma, M., 1997. Siberian Traps. In: Mahoney, J.J., Coffin, M.F. (Eds.), Large Igneous Provinces: Continental, Oceanic, and Planetary Flood Volcanism. American Geophysical Union Monograph. pp. 273–295.
Shirey, S.B., 1997. Re–Os isotopic compositions of Midcontinent rift system picrites: implications for plume-lithosphere interaction and enriched mantle sources. Can. J. Earth Sci 34, 489–503.
Smoliar, M.I., Walker, R.J., Morgan, J.W., 1996. Re–Os ages of Group IIA, IIIA, IVA and IVB iron meteorites. Science 271, 1099–1102.
Song, X.Y., Zhou, M.F., Hou, Z.Q., Cao, Z.M., Wang, Y.L., Li, Y.G., 2001. Geochemical constraints on the mantle source of the upper Permian Emeishan continental flood basals, southwestern China. Int. Geol. Rev 43, 213–225.
Taylor, S.R., McLennan, S., 1995. The geochemical evolution of the continental crust. Reviews of Geophysics 33, 241–265.
Tejada, M.L.G., Mahoney, J.J., Castillo, P.R., Ingle, S.P., Sheth, H.C., Weis, D., 2004. Pin-pricking the elephant: evidence on the origin of the Ontong Java Plateau from Pb–Sr–Hf–Nd isotopic characteristics of ODP Leg 192 basalts. In: Fitton, J.G., Mahoney, J.J., Wallace, P.J., Saunders, A.D. (Eds.), Origin and Evolution of the Ontong Java Plateau. Spec. Publ, vol. 229. Geological Society, London, pp. 133–150.
Walker, R.J., Carlson, R.W., Shirey, S.B., Boyd, F.R., 1989. Os, Sr, Nd and Pb systematics of southern African peridotite xenoliths: implications for the geochemical evolution of subcontinental mantle Geochim. Cosmochim. Acta 53, 1583–1596.
Walker, R.J., Storey, M., Kerr, A.C., Tarney, J., Arndt, N.T., 1999. Implications of ^{187}Os isotopic heterogeneities in a mantle plume: evidence from Gorgona Island and Curaçao. Geochim. Cosmochim. Acta 63, 713–728.
Walker, R.J., Morgan, J.W., Hanski, E.J., Smolkin, V., 1997. Re–Os systematics of Early Proterozoic ferropicrites, Pechenga Complex, NW Russia: evidence for ancient ^{187}Os enriched plumes. Geochim. Cosmochim. Acta 61, 3145–3160.
Walker, R.J., Morgan, J.W., Horan, M.F., 1995. ^{187}Os enrichment in some mantle plume sources: evidence for core–mantle interaction. Science 269, 819–822.
Walker, R.J., Morgan, J.W., Horan, M.F., Czamanske, G.K., Krogstad, E.J., Likhachev, A.P., Kunilov, V.A., 1994. Re–Os isotopic evidence for an enriched-mantle plume source for the Norils-type ore-bearing intrusions, Siberia. Geochim. Cosmochim. Acta 58, 4179–4198.
Wang, D.H., 2001. Basic conception, classification, evolution of mantle plume and large scale mineralization—probe into southwestern China. Earth Sci. Front 8, 67–72 (in Chinese with English abstract).
Wang, C.Y., Zhou, M.F., Keays, R.R., 2006. Geochemical constraints on the origin of the Permian Baimazhai mafic–ultramafic intrusion, SW China. Contrib. Mineral. Petrol. 152, 309–321.
Widom, E., Hoernle, K.A., Shirey, S.B., Schmincke, H.U., 1999. Os isotope systematics in the Canary Islands and Madeira: lithospheric contamination and mantle plume signatures. J. Petrol 40, 279–296.
Widom, E., Shirey, S.B., 1996. Os isotope systematics in the Azores: implications for mantle plume sources. Earth Planet. Sci. Lett 142, 451–465.
Xiao, L., Xu, Y.G., Mei, H.J., Zheng, Y.F., He, B., Pirajno, F., 2004. Distinct mantle sources of low-Ti and high-Ti basalts from the western Emeishan large igneous province, SW China: implications for plume-lithosphere interaction. Earth Planet. Sci. Lett 228, 525–546.
Xu, J.F., Suzuki, K., Xu, Y.G., Mei, H.J., Li, J., 2007. Os, Pb, and Nd isotope geochemistry of the Permian Emeishan continental flood basalts: insights into the source of a large igneous province. Geochim. Cosmochim. Acta 71, 2104–2119.
Xu, Y., He, B., Chung, S.L., Menzies, M.A., Frey, F.A., 2004. Geologic, geochemical, and geophysical consequences of plume involvement in the Emeishan flood-basalt province. Geology 32, 917–920.
Xu, Y., Chung, S., Jahn, B., Wu, G., 2001. Petrologic and geochemical constraints on the petrogenesis of Permian-Triassic Emeishan flood basalts in southern China. Lithos 58, 145–168.
Yan, M.C., Chi, Q.H., Gu, T.X., Wang, C.S., 1997. Chemical compositions of continental crust and rocks in eastern China. Geophysical and Geochemical Exploration 21, 452–459.
Zhang, Z.C., Mahoney, J.J., Mao, J.W., Wang, F.S., 2006a. Geochemistry of picritic and associated basalt flows of the western Emeishan flood basalt province. China. J. Petrol 47, 1997–2019.
Zhang, Z.C., Mao, J.W., Wang, F.S., Pirajno, F., 2006b. Native gold and native copper grains enclosed by olivine phenocrysts in a picrite lava of the Emeishan large igneous province. Am. Miner 91, 1178–1183.
Zhang, Z.C., Wang, F.S., 2002. Geochemistry of the two types of basalts of the Emeishan basaltic province: evidence for mantle plume–lithosphere interaction. Acta Geol. Sin 76, 229–238.
Zhi, X.C., Qin, X., 2004. Re–Os isotope geochemistry of mantle-derived peridotite xenoliths from eastern China: constraints on the age and thinning of the lithosphere mantle. Acta Petrol. Sin 20, 989–998.
Zhong, H., Zhu, W.G., 2006. Geochronology of layered mafic intrusions from the Pan-Xi area in the Emeishan large igneous province, SW China. Mineral Deposita 41, 599–606.
Zhou, M.F., Arndt, N.T., Malpas, J., Wang, C.Y., Kennedy, A.K., 2008. Two magma series and associated ore deposit types in the Permian Emeishan large igneous province, SW China. Lithos 103, 352–368.
Zhou, M.F., Malpas, J., Song, X.Y., Robinson, P.T., Sun, M., Kennedy, A.K., Lesher, C.M., Keays, R.R., 2002. A temporal link between the Emeishan large igneous province (SW China) and the end-Guadalupian mass extinction. Earth Planet. Sci. Lett 196, 113–122.